10.48047/jocaaa.2023.31.04.47

Creating a smart water spray cooling system using an Arduino to cool a solar panel in a 40KWp hybrid solar wind power plant, which uses a 22 kg cm bipolar stepper motor water pump with a 4-amp motor to enhance the system's power output.

***Dinesh Paswan*[1], Dr. Vikas Kumar Aharwal[2]**

[1]Department of Electrical Engineering,, DR. A.P.J.Abdul Kalam University,Indore,India, Indore-Dewas Bypass Road, Village- Arandia, P.O. Vijay Nagar, Indore, Indore (M.P.) – 452010, M.P, India, Email addresses: dineshpaswan2@gmail.com (Dinesh Paswan),

[2]Department of Electrical Engineering,, DR. A.P.J.Abdul Kalam University,Indore,India, Indore-Dewas Bypass Road, Village- Arandia, P.O. Vijay Nagar, Indore, Indore (M.P.) – 452010, M.P, India, Email address: *aharwal.vikas@gmail.com*

Abstract

The main goal of our study was to explore and expand an Arduino-based smart water spray cooling method and evaluate its impact on the performance of a PV panel in different weather conditions in Bankura. The results showed that this method the standard PV model without cooling, leading to more effective outcomes. The cooling process was intentionally set up from 10 A. M. to 3 P. M. The findings revealed that the system's power output increased from 23 KWp to 25 KWp, which is an improvement of about 10%. It was also observed that the panel temperature dropped significantly from an average of 76°C to 25°C. The program was written in a way that activates the cooling system when the PV cell temperature rises above 25°C.The module V_{max} decreases by approximately 0.5%per degree centigrade so maintain the photovoltaic We have developed Arduino based smart water spray cooling technique where we can control 1.8^0 Cool Stepper Motors High Torque Hybrid, BH57 SH 81 - 4004 AF, NEMA 23(57 mm) Frame size, Bipolar (4 leads), Holding Torque 22 kgcm (2.2 Nm), Current per phase 4 Amp, Motor length 81 mm, 300mm Wire Length, Operating Voltage 24 - 48 VDC,With Flat Milled Shaft. For complete details please view Technical using a microcontroller based temperature controller. As the PV cell temperature increases above 25ºC, the module V_{maxp} decreases by approximately 0.5% per degree C so maintenance

10.48047/jocaaa.2023.31.04.47

the photovoltaic panels is very important. The microcontroller programming is set up so that the water spray will turn on automatically for 15 minutes when the PV cell temperature goes above 25 degrees Celsius, and it will turn off automatically when the temperature drops below 25 degrees Celsius. This helps improve the immediate positive power output.

Keywords: Solar energy, on grid power plant, size of plant, Educational Institutions, Load

---

1. Introduction: Global warming is a major problem that affects the entire world. To address this, we need to make big changes by using renewable energy sources. These are energy sources that can be renewed or replaced within a person's lifetime. Examples include solar, wind, water, tides, and geothermal energy. Solar panels are not as efficient when they get too hot. While solar PV systems are great for producing electricity and have no moving pa rts, they can lose some efficiency in high temperatures. A standard solar panel has 72 solar cells, which are connected either in series or parallel. Thin-film panels are made with gallium arsenide and
are less sensitive to heat. Some systems use water spray to cool panels, which can carry a current of 8 amps. There are four types of cooling methods available in the market. One of them is not usually provided by the manufacturer but arranged by the customer. It is easier to implement but
not very efficient. By adapting different cooling technologies based on local geographical conditio ns, we can reduce the panel temperature from 76°C to as low as 27°C, 30°C, and 26°C for front, side,
both front and back cooling are used, active power production can increase by up to 10%. Our proposed technology is more effective than these methods. It can lower the panel temperature from 76°C to 25°C. The main goal of our study was to develop an Arduino-based smart water spray cooling method and evaluate its impact on the performance of the PV panel in different weather conditions in Bankura. We compared the results with a normal PV model that was not cooled. The experiment was conducted between 10 AM and 3 PM. The result showed that the active power capacity increased from 23 KWp to 25 KWp, which is an improvement of about 10%. The panel temperature was reduced from an average of 76°C to 25°C. The programming is designed in such a way that when the PV cell temperature goes above

10.48047/jocaaa.2023.31.04.47

25°C, the Vmax of the module drops by approximately 0. 5% per degree Celsius. To maintain the efficiency of the photovoltaic system, we developed an Arduino-based smart water spray cooling technique. This setup uses a 1. 8° Cool Stepper Motor High Torque Hybrid, BH57 SH 81 - 4004 AF, NEMA 23 (57 mm) Frame size, Bipolar (4 leads), with a holding torque of 22 kgcm (2. 2 Nm), current per phase of 4 Amp, a motor length of 81 mm, 300 mm wire length, and an operating voltage of 24–48 VDC, with a flat milled shaft. For more details, please refer to the technical specifications, which use a microcontroller-based temperature control system. As the PV cell temperature rises above 25°C, the module Vmax decreases by approximately 0. 5% per degree Celsius. Therefore, maintaining the panel temperature is essential for the efficiency of the photovoltaic system. The programming is set so that water spray turns on for 15 minutes when the PV cell temperature exceeds 25°C and turns off automatically when it drops below 25°C to improve active power. Front cooling, as well as front and back cooling, are also effective methods. Our technique is better than floating PV modules because it can manage the panel temperature without being affected by the atmospheric temperature. There is limited research on the impact of water spray techniques on the performance of a 50 KWp grid-tied solar PV system, so we have developed this proposed method to enhance the active power using an Arduino-based smart water spray cooling technique on the photovoltaic panel. This helps improve the active power of a 50 KWp grid-tied solar system using an induction motor water pump. The output of the solar PV system depends on the solar radiation it receives, not on temperature. Increasing the solar radiation can improve the output of the system. High temperatures can reduce the efficiency of solar cells, especially when the cell temperature exceeds 25°C. Only 15 to 20% of sunlight is used to generate electricity, and the rest is wasted. The efficiency of the solar cell can decrease by about 0. 5% for every degree above 25°C. The open circuit voltage of the solar cell also depends on the intensity of the light. The temperature of the solar cells is influenced by the climate and can be affected by direct or indirect shading. Atmospheric wind can help lower the solar cell temperatu re. Sometimes, water and air are used together as coolants. In many places, the temperature is measured in Celsius. We have installed an SR motor pump to maintain a hybrid power plant and solar module temperatures for higher efficie

10.48047/jocaaa.2023.31.04.47

ncy. These pumps are connected throughout the panels, which help absorb heat from the solar panels. Water is pumped through the system to cool the panels. Phase change materials have a unique quality; they absorb heat during the day and can release it when the environment is cooler. Keeping the solar cell temperature below the rated level can extend the lifespan of the panels from 25 years to 45 years. The experimental results showed that maintaining lower PV temperatures can improve th e efficiency of a floating PV array by 27% compared to 8. 18% when using a thermos iPhone. A solution using an aluminum water jacket is robust but expensive..

Water circulatory pipes are reduce the PV module temperature from 76°C to 25°C. Thermos iPhone passive cooling system Lowers by adapting other cooling technology like back cooling better than floating PV module because Here, we can't fans and water pumps are used as an active coolants [17]. There are three passive cooling techniques.

2. Methodology

The output voltage of the Arduino is 5 volts. We can control various types of loads such as lights, fans, and water pumps that operate at voltages between 120 V and 240 V by using a relay. The relay can be turned on or off based on the program running on the embedded system. We have installed a program on the Arduino board. If the temperature sensor detects a temperature above 25 degrees, a 5V supply is sent to activate the 5V-operated relay for 15 minutes. The relay then connects the water pump motor to the external AC power source. After the relay is turned on for 15 minutes, a delay of about 12 hours is set. We use an SPD-05V SL-C relay. The DIY temperature sensor measures temperatures up to 25 degrees Celsius. The maximum voltage output of the solar module decreases by roughly 0. 5% for every 1 degree rise in temperature above 25 degrees. This is nearly impossible during the summer season because the average temperature in Bankura often goes above 37 degrees.

1.1. Flow Chart

The SR motor pump is operated fully automatically with the help of microcontroller board Arduino, Here, a 5V relay is used to control turn ON/OFF a High Torque Hybrid, BH57 SH 81

10.48047/jocaaa.2023.31.04.47

- 4004 AF, NEMA 23 (57 mm) Frame size, Bipolar (4 leads), with a holding torque of 22 kgcm (2. 2 Nm), current per phase of 4 Amp, a motor length of 81 mm, 300 mm wire length, and an operating voltage of 24–48 VDC, with a flat milled shaft.

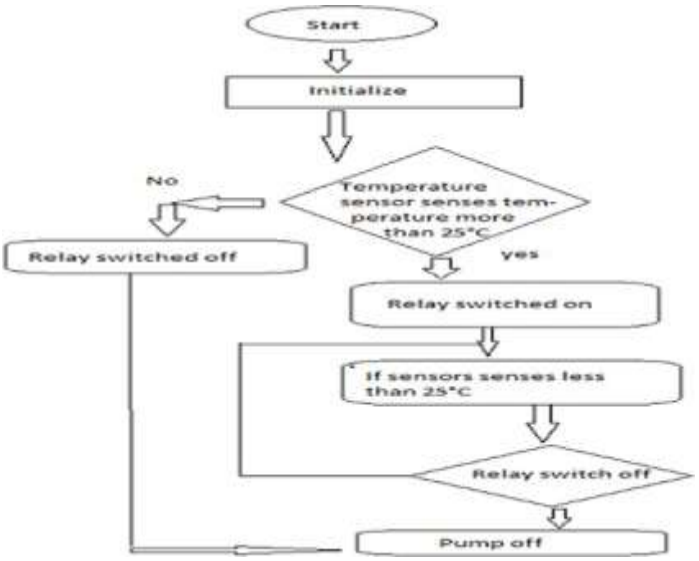

Figure 1: Flowchart of entire set-up

A Bipolar stepper motor pump with the help of temperature sensor.

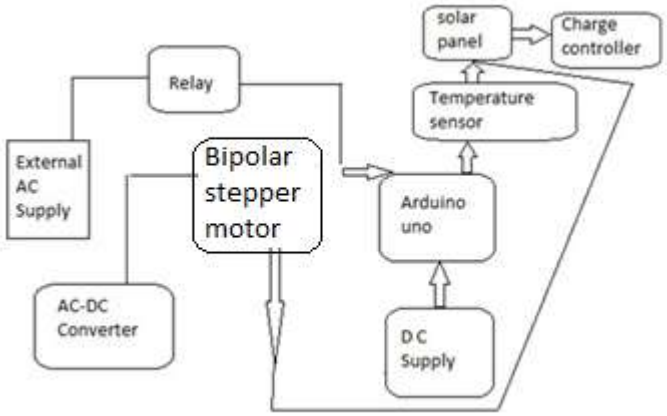

Figure 2: Block diagram of overall set-up

A program is burned to operate the relay. Bipolar stepper pump will switch on whenever a temperature sensor will sense more than 25 degree centigrade. The temperature sensor is connected to solar panel [15]. DC power is fed to the Arduino Uno circuit for proper operation. The relay is connected to an external AC source. AC supply is fed to AC to DC converter to create some DC voltage which is fed to power circuit of SR motor pump for its smooth

10.48047/jocaaa.2023.31.04.47

operation

1.1 Circuit Implementation

The laptop is connected to one end of the USB cable, and the other end is plugged into

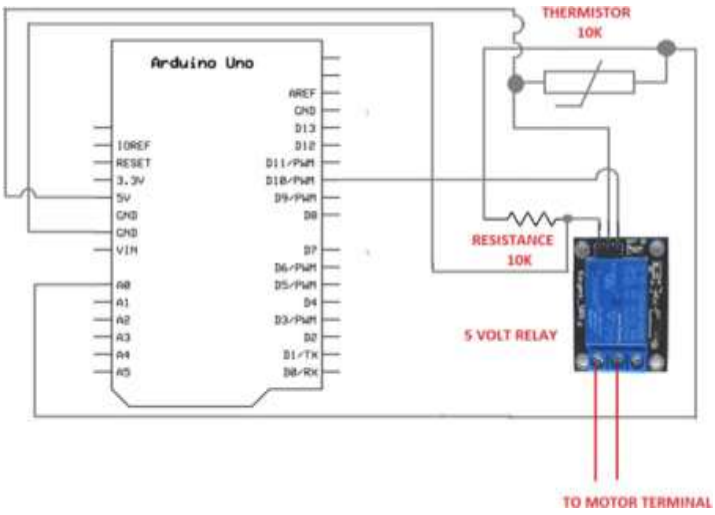

a USB port. The relay has four terminals: Vcc, VRD, Vin, and two outputs. The two output terminals are connected to a motor, with one connected to the power supply (Vcc) and the other to the ground (Gnd). The temperature sensor's output, which is labeled A0, is connected to the positive terminal. The other terminal of the sensor is connected to the 5V power supply of the Arduino Uno board, and the third terminal is connected to the common ground. The relay is rated for a voltage range of 120V to 240V DC. The microcontroller has six analogue input pins, labeled A0 to A5, each with 10-bit resolution. Some of the pins have specific functions, such as TX for transmitting TTL signals and RX for receiving data.

Figure 3: Pin diagram of Microcontroller circuit

Special pin functions-

Digital write(), pin mode(), and digital read() are used here. The microcontroller ATMega8U2 is used. Digital pins are connected to outputs such as LEDs, relays,
and LCDs. Analog pins are used for input sensors like temperature sensors. Only a 5V supply is us ed for both input and output components. There is a power jack to supply power to the Arduino. A 9V battery is connected through

10.48047/jocaaa.2023.31.04.47

the power port. There is a USB port for uploading the program. All the legs are connected to the ATmega8U2 USB to TTL chip. Pins 3, 5, 6, 9, 10, and 11 support PWM. The analogWrite() function is used on these pins. Pins 11 (MOSI), 12 (MISO), and 13 (SCK) help in connecting the SPI library. The Adriano board has an analog reference (AREF), TWI (Two Wire Interface) with SCL, and SDA. It also has analog input with a special reference. The IDE includes a periodic examiner that allows data to be sent to the board through RX and TX. LEDs flash to show data transmitted via USB. To upload the program, we need to reset the Uno board using the ATmega8U2/16U2 microcontroller, which connects the reset line through a 100 nanofarad capacitor. It acts as a smart gateway for flexible data access from any hardware system. The boot loader blocks data after the connection is established. To perform the required coding and set up the proper configuration with the Arduino Uno board, the IDE (Integrated Development Environment) is used. The BAUD RATE (uploading speed) is set to around 9600, and it uses COM5. It is a microcontroller that uses an IOT platform.

1.1.1 Software Implementation*:*

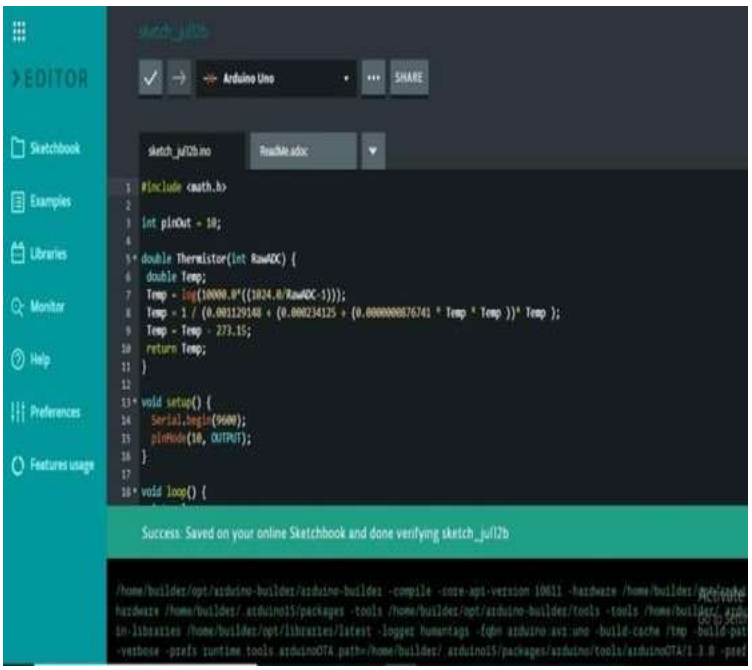

Figure 4: successful compilation

10.48047/jocaaa.2023.31.04.47

It is essentially a request that spans both C and C++ manifestos. It involves mathematical pins on Uno. It works on OS X or Linux, and it performs each time it is used to address a suitable condition. The equating of two position controls will be triggered. The Arduino Uno board is designed to work with an operating system that runs on a related microcontroller. The DTR of the AT-Mega8U2/16U2 is collected along with a faulty line from the ATmega328 through a 100 Nano farad capacitor. When this line is detected (pressed),
the reset line drops long enough to reset the chip [27]. This setup has different implications when the Uno is being used with a calculating running Mac 3. 3 automatic (operating system) changed. Instead of needing a physical press of
the relocation knob before transferring data to a server, when files are being sent through the USB-to-serial chip and USB network to the computing device (but not using serial communication on pins 0 and 1). A Software Serial library allows serial communication on one pin that is created from a spreadsheet (through USB) [25].

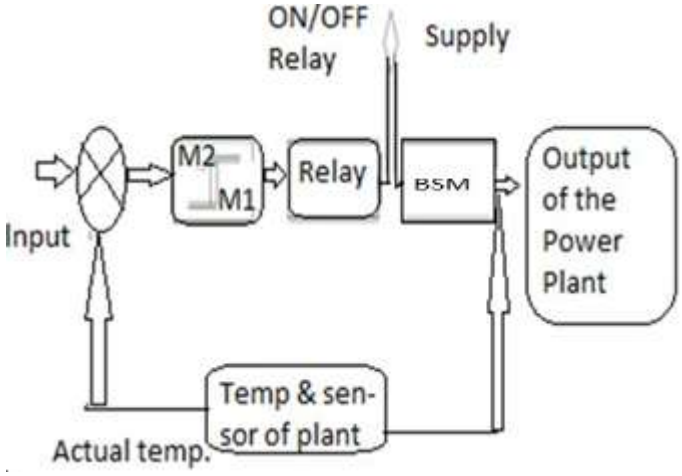

Figure 5: Block diagram of two position Control strategy of BSM

10.48047/jocaaa.2023.31.04.47

Two position control method

In this type of control the output of controller is quickly changed to either a maximum or minimum value depending upon weather the controlled variable (b) is greater or less than the set point or in other words depends upon the actuating error signal (e) . The minimum value is usually zero

M1 = Controller maximum output (Pump relay switch is OFF to ON)

M2 = Minimum value of output of controller (Pump relay switch is to ON to OFF)

E = Actuating error signal or deviation

m = M1, when e≤0 (reference temperature is more than set temp value)

m =M2 when e≥0 ((reference temperature is less than set temp value)

In standard full-step operation, quadrature (out of phase by 90°) bipolar currents (Figure 1) energize the Windings of a bipolar stepper motor. One step occurs at each change of direction of both winding current, and the motor steps at four times the frequency of the currents. The ideal winding currents of Figure 1 exhibit infinite slew rates. Ideally, each phase contributes a sinusoidal torque:

T1 = −i1 Tsin(Nθ) and (1)

T2 = i2 Tcos(Nθ), (2)

with the winding currents, i(t), in amps and the torque constants, -Tsin(N•θ) and Tcos(N•θ), in newton•centimeters per amp. θ represents the angular displacement of the rotor relative to a stable detent(zero torque) position. N represents the number of motor poles; that is, the number of electrical cycles per Mechanical cycle or revolution. N•θ, therefore, represents the electrical equivalent of the mechanical rotor position. The torque contributions add directly to yield a total torque of: Tt = T1 + T2 = T (i2 cos (Nθ) − i1 sin (Nθ)). (3)Integrating (3) over a full period of one of the torque constants and multiplying the result by the reciprocal of that period gives the average torque generated by the motor. Assuming ideal square wave winding currents and sinusoidal torque constants (Figure 2), the motor generates an average torque of:

$$T_{avg} = \frac{1}{2\pi}\left[\int_{o}^{2\pi} - i_1\, T\sin(N\theta)\, dN\theta + \int_{o}^{2\pi} i_2\, T\cos(N\theta)\, d\, N\theta\right] =$$

10.48047/jocaaa.2023.31.04.47

$$= \frac{2}{\pi} I_{rated} T \cos\phi.$$

In open loop applications, Φ adjusts automatically to match the average torque generated by the motor with that required to execute a motion task. When the winding currents and their respective torque constants are in phase (Φ is zero), the motor generates the maximum average

10.48047/jocaaa.2023.31.04.47

Torque or *pull-out torque*

$$T_{pull\text{-}out} = T_{avg\,(max)} = \frac{2}{\pi} I_{rated}\, T.$$

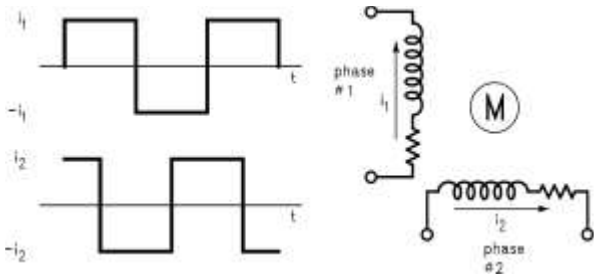

Figure 1. Ideal Quadrature Currents Drive the Windings of a Bipolar Stepper Motor

So, I=0 (Phase current will be zero) lesser torque at high speed Its characteristics just like DC series motor When relay turn off or when disconnected with supply if atmospheric temperature goes less than the set Temperature i.e. 250C Circuit output during testing of nature of logic pulses for anti-clockwise rotation of the rotor

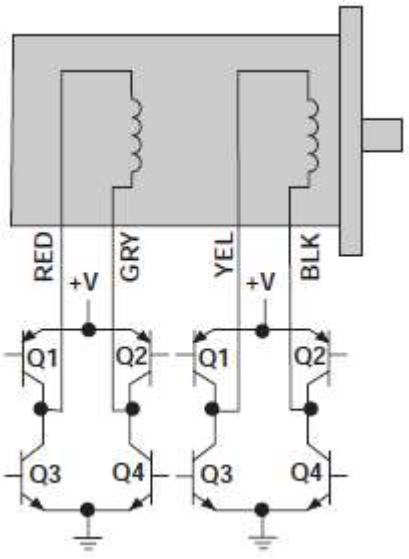

The stator flux with a bipolar winding is reversed by reversing the current in the winding. It requires a push-pull Bipolar drive as showman Fig. 14. Care must be taken to design the circuit so that the

10.48047/jocaaa.2023.31.04.47

transistors in series do not short the power supply by coming on at the same time. Properly operated, the bipolar winding gives the optimum motor performance at low-to-medium step rates.

BIPOLAR

	Step	Q_1-Q_4	Q_2-Q_3	Q_5-Q_8	Q_6-Q_7	
CW ROTATION	1	ON	OFF	ON	OFF	CCW ROTATION
	2	ON	OFF	OFF	ON	
	3	OFF	ON	OFF	ON	
	4	OFF	ON	ON	OFF	
	1	ON	OFF	ON	OFF	

Flux is reversed in each coil bobbin assembly by sequentially grounding ends of each half of the coil winding. The use of a unipolar winding, sometimes called a *bifilar winding*, allows the drive circuit to be simplified. Not only are half as many power switches required (4 vs. 8), but the timing is not as critical to prevent a current short through two transistors as is possible with a Bipolar drive.

Table.2. Logic output for clockwise rotation of rotor

	specification	Bipolar stepper motor
Sl no	Rated Voltage	2
1	Rated current	4 Amp
2	Resistance per phase	0.5
3	Inductance per phase	1.4
4	Holding Torque Nm	2.2
5	Rotor Inertia	500
6	Weight	1.5
7	No of Lead	4
8	Operating Voltage	24-48V

3. Experimental results and discussion

General means The committee was proven on a terrestrial locale in Bankura, West Bengal .Measurements were supported from 10 AM to 15 PM. During the succession of calculations, the surrounding air hotness categorized from 25 ◦C and until 44◦C During the series of measurement the solar cell temperature ranged from 23◦ C to 76◦ C, Here 76◦ C is the total module temperature During the measurement series, air velocities were under 20 m/s (Yearly average wind velocity) and inlet water temperature was approximately constant, at around 28 ◦C (average measured water inlet temperature from the pipeline).

10.48047/jocaaa.2023.31.04.47

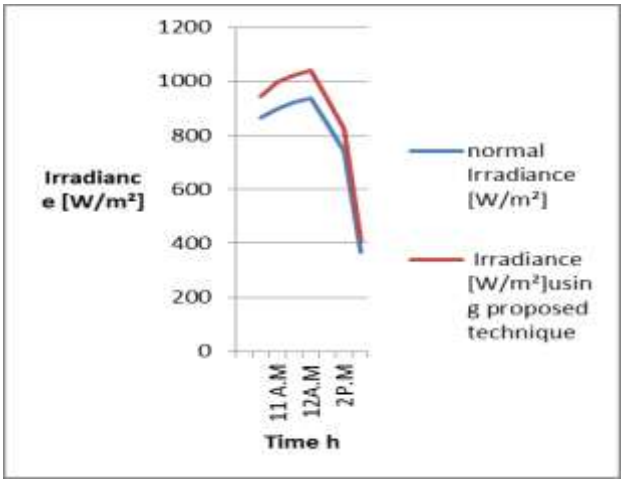

Figure 16: indicates Irradiation variation during the measurement period

During the process of calculations, the solar beam was measured to range from 850 W/m² to 1150 W/m². We can confidently say that before using our smart water spray cooling method, the maximum irradiation was 850 W/m². After applying the Arduino-based smart water spray cooling system, the irradiation increased up to 1150 W/m². We can clearly see that irradiation is directly related to the sun's energy production. The irradiation increased by 26%. A significant amount of improvement was affected by dust particles on the surface of the solar panels. Some of the solar beam was blocked by the dust. The module temperature was very high, nearly reaching 76°C, while the cell temperature ranged from 44°C to 25°C. The maximum average energy output of the non-cooled panel was 27. 9 W. In the case of the PV panel, the maximum average energy output increased to 32 W after applying our cooling method. When both front and rear cooling were used together on the PV panel, there was a significant increase in the energy output compared to the non-cooled panel, with a total increase of 15%. The highest average increase in energy output was achieved with a water spray flow rate of 225 liters per hour. The average energy efficiency of the non-cooled PV panel was 16%, while the maximum average efficiency achieved was 18%. Therefore, the overall increase in energy efficiency was 2% compared to the average efficiency of the non-cooled PV panel.

10.48047/jocaaa.2023.31.04.47

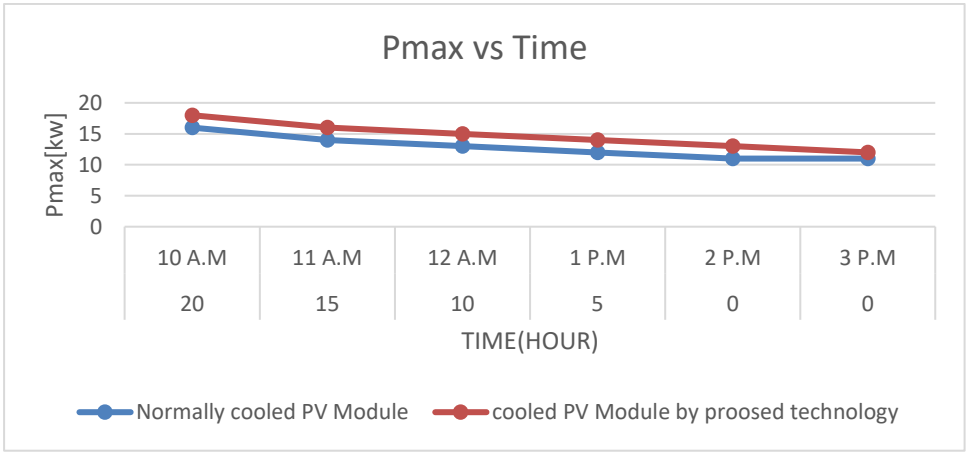

Figure 17: indicates ambient temperature variation during the measurement period

Water spray cooling method effect on PV committee hotness decline Achieved temperature decline middle from two points the case of non-cooled PV committee and cooled PV committee (indifferent cooling regimes), was proved in Fig. (the dossier bestowed in Fig.7 are for cosmic irradiation levels at about 850–1150 W/m2, encircling air hotness at about 24–44 ˚C and water spray hotness at around 25 ˚C). In the case of the non-cooled PV committee,.

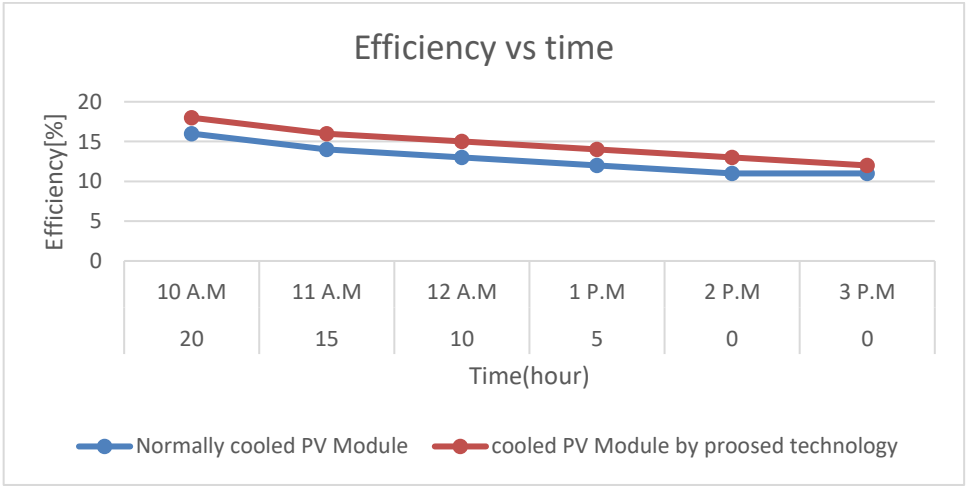

Figure 18: indicates ambient temperature variation during the measurement period

During the succession of calculation, the battery powered by the sun temperature categorized

10.48047/jocaaa.2023.31.04.47

From 23°C to 76°C, 76°C represents the overall heat level of the system. On the other hand, by using the water spray cooling method, it was possible to bring the temperature down to just below 25°C, which is a significant drop. The greatest reduction in system heat was achieved when both cooling methods were used together. The cooling effect influences the system's energy production capacity and electrical efficiency. Figures 8 and 9 show the energy output and efficiency against time for various cooling methods, based on a series of experiments conducted throughout the measurement period. In the case where both parts of the system were cooled together, the maximum average energy efficiency achieved was 8. 11%. Therefore, the overall energy efficiency increased by 17. 37% compared to the average efficiency of the non-cooled PV system. It is clear that improving the system's efficiency and achieving the highest average temperature reduction is possible when both parts of the PV system are cooled together with water.

Nomenclature

PUF Plant utilization factor

CF Utilization factor

P power (KW)

E energy rate (KWh)

DF Diversity factor

LF Load factor

PWM Pulse width modulation

Greek symbols

Ψ Flux

E Efficiency

Θ Rotor position angle

10.48047/jocaaa.2023.31.04.47

4. Conclusion & scope for future work

In this paper method was projected and tentatively tested on a Polycrystalline Photovoltaic committee indifferent weather environments of Bankura. Experimentally There is an active increase in Active capacity of PV photovoltaic cell from 23 KWp to 27 KWp. It increases overall plant efficiency about 10%. The average solar module temperature was diminished from 76˚C to 25˚C and hostile attainable committee hotness was limited to 25˚C, finally, in accordance with win tentatively results. It may be concluded that the projected method has received a approving effect on committee output conduct and it is more a possible individual

5. REFERENCES

[1] B. Sreewirote, and M. Leelajindakrairerk, "Design and development of solar water pump," in: 19th Int. Conf. Electr. Mach. Syst., IEEE, Chiba, Japan, 2016: pp. 1–5. 3) S. Wolfert, L. Ge, C. Verdouw, and M. J.Bogaardt, " Big data in smart farming – a review," *Agric. Syst.*, **153** 6980(2017).doi:https://doi.org/10.1016/j.agsy. 2017.01.023

[2] Assessment of Wind Energy Potentiality at Ajloun, Jordan Using Weibull Distribution Function Mohanad Al-Ghriybah1,*Department of Renewable Energy Engineering, Faculty of Engineering, Isra University, Amman, Jordan , Novel Carbon Resource Sciences & Green Asia Strategy EVERGREEN Joint Journal, Vol. 09, Issue 01, pp10-16, March 2022Carbon Resource Sciences & Green Asia Strategy Mohd Faizal Mohideen Batcha2, Kamil Abdullah2, , Vol. 08, Issue 02, pp271-279, June 2021

[3] Technical Feasibility Analysis of Wind Energy Potentials in two sites of East Malaysia: Santubong and Kudat Terence Clinton Rudien1, Djamal Hissein Didane2,*, Sofian Mohd3, Bukhari Manshoor2, Sami Al-Alimi1EVERGREEN Joint Journal of Novel Carbon Resource Sciences & Green Asia Strategy Mohd Faizal Mohideen Batcha2, Kamil Abdullah2, , Vol. 08, Issue 02, pp271-279, June 2021

[4] H. Watanabe and T. Maruyama, "Residential preference transitions of disaster victims: A case using three-wave panel data in Mashiki following the 2016 Kumamoto earthquake in Japan," Int. J. Disaster Risk Reduct., vol. **54**, pp. 1–8 (2021).

[5] Technical Feasibility Analysis of Wind Energy Potentials in two sites of East Malaysia:

10.48047/jocaaa.2023.31.04.47

Santubong and Kudat Terence Clinton Rudien1, Djamal Hissein Didane2,*, Sofian Mohd3, Bukhari Manshoor2, Sami Al-Alimi1EVERGREEN Joint Journal of Novel

[6] Techno-Economic Comparative Analysis between Grid Connected and Stand-Alone Integrated Energy Systems for an Educational Carbon Resource Sciences & Green Asia Strategy, Vol. 07, Issue 03, pp382-395, September, 2020.

[7] EVERGREEN Joint Journal of Novel Carbon Resource Sciences & Green Asia Strategy Wind Lens Performance Investigation at Low Wind Speed M. M. Takeyeldein1, *, Tholudin Mat Lazim1, Iskandar Shah Ishak1, Nik Mohd, N.A.R1, and Essam Abubakr Ali, Vol. 07, Issue 04, pp481-488, December 2020

[8] Key Factors of Solar Energy Progress in Bangladesh until 2017 Marzia Khanam1,2*, 2 EVERGREEN Joint Journal of Novel Carbon Resource Sciences & Green Asia Strategy,Muhammad Faisal Hasan1, Takahiko Miyazaki1,2, Bidyut Baran, Saha2, Shigeru Koyama1, , Vol. 05, Issue 02, pp.78-85, June 2018

[9] Harry Ku (1966) Notes on the Use of Propagation of Error Formulas. J Res Natl Bureau Stand C Eng Instrum 70C(4):263–273 Singh GK (2013) Solar power generation by PV technology: a review. Energy 53:1–13. https ://doi.org/10.1016/j.energ y.2013.02.057 .Schiro F, Benato A, Stoppato A, Destro N (2017)

[10] R outbib, N Moubayed, N. Karani, and "classification of different MPPT Techniques and General review " sustainable energy reviews and renewable " Vol. 76, PP 163-175, 20Fakouriyan, S., Saboohi, Y. & Fathi, A. Experimental analysis of a cooling system effect on photovoltaic panels' efficiency and its preheating water production. *Renew Energy* **134**, 1362–1368 (2019). 17

[11] D. Keerthika, A. N. Arvindan and "Experimental investigation of remote control via Android smart phone of arduino-based automated irrigation system using moisture sensor," 2016 3rd International Conference on Electrical Energy Systems (ICEES), Chennai, 2016, pp. 168-175pt.

Y.T. Abirham, K. Thu, T. Miyazaki, and N. Takata, "Comparative study of thermal

[11]water pumping cycles," *Evergreen*, **8** (*1*) 239–248 (2021). doi:10. 5109/4372284.

[12]S. Krauter, ," Solar Energy Materials & Solar Cells, "Increased electrical yield via water flow over the front of photovoltaic 625 panelsvol. 82, no. 1-2, pp. 131-137, May 2004.105, pp. 14 July 2014.

.[13]N. Arcuri ,F. Reda, , , M. De Simone, evaluations of 627photovoltaicpanels cooled by water

10.48047/jocaaa.2023.31.04.47

and air," Solar Energy, vol. driven ventilator to enhance a photovoltaic cell power In- stitute Siva Subrahmanyam Mendu1,*, Padmaja Appikonda2, Anil Kumar Emadabathuni3, Naresh Koritala2EVERGREEN Joint Journal of Novel "Energy and thermo-fluid-dynamicP. Valeh-E-Sheyda, M. Rahimi, generation," Energy and Buildings, vol. 63073, pp. 115-119, Apr. 2014.

[14] I. Odeh, Y.G. Yohanis, and B. Norton, "Influence of pumping head, insolation and pv array size on pv water pumping system performance," *Sol. Energy*, **80** (*1*) 51–64 (2006).doi:https://doi.org/10.1016/j. solener.2005.07.009. Arcuri Engineering, vol. 3, no. 1, pp. 97-101, 617 Sept. 2013.

[15] Harry Ku (1966) Notes on the Use of Propagation of Error Formulas. J Res Natl Bureau Stand C Eng Instrum 70C(4):263–273 Singh GK (2013) Solar power generation by PV technology: a review. Energy 53:1–13. https ://doi.org/10.1016/j.energ y.2013.02.057

[16] NK. Nawandar, and V.R. Satpute, "IoT based low cost and intelligent module for smart irrigation system," *Comput. Electron. Agric.*, **162** (*May*) 979–990 (2019). doi:10.1016/j.compag.2019.05.027.

[17]H. G. Teo, P. S. Lee, M. N. A. Hawlader, "An active cooling system for photovoltaic 635 modules," Applied Energy, vol. 90, no. 1, pp. 309-315, Feb. 2012.

[18] World Bank, ESMAP & SERIS. Where Sun Meets Water : Floating Solar Market Report - Executive Summary. 1–24 (2018).

[19] Hachicha, A. A., Ghenai, C. & Hamid, A. K. Enhancing the Performance of a Photovoltaic Module Using Different Cooling Methods. *International Journal of Energy and Power Engineering* **9**, 1106–1109 (2015).

[20] Schiro F, Benato A, Stoppato A, Destro N (2017) Improving photovoltaics efficiency by water cooling: modelling and experimental approach. Energy 137:798–810. https ://doi. org/10.1016/j.energ y.2017.04.164

[21] Hidayat, F. Peningkatan Efisiensi Elektrik Modul Surya Menggunakan Bahan Berubah Fasa Maximum Power Point Tracking (MPPT). **I**, 154–165 (2013).

[22] Sutanto, B. & Indartono, Y. S. Computational fluid dynamic (CFD) modelling of floating photovoltaic cooling system with loop thermosiphon. *AIP Conf Proc* **2062**, 2–7 (2019).

[23] Nianyong Z, Fujiang C, Yuchun C, Mengmeng C, Wang Yu (2017) Experimental investigation on the performance of a water spray cooling system. Appl ThermEng 112:1117 1128.https://doi.org/10.1016/j.applt herma leng.2016.10.191

10.48047/jocaaa.2023.31.04.47

[24] Strategy, G. A. A Numerical Investigation of an Offshore Overhead Power Transmission System. *Evergreen* **09**, 636–644 (2022).

[25] B. Aksu I. Ceylan, A.E. Gürel, H. Demircan,Cooling of a photovoltaic module with temperature controlled solar collector, Energy .Build.72(2014)96101,https://doi.org/10.10